J. Plasma Physics (2009), *vol.* 75, *part* 3, *pp.* 413–431.
doi:10.1017/S0022377808007721 Printed in the United Kingdom

DIA and DA solitary waves in adiabatic dusty plasmas

A. A. MAMUN[1], N. JAHAN[1] and P. K. SHUKLA[2]

[1] Department of Physics, Jahangirnagar University, Savar, Dhaka-1342, Bangladesh (mamun_phys@yahoo.co.uk)

[2] Fakultät für Physik und Astronomie, Ruhr-Universität Bochum, D-44780 Bochum, Germany

(Received 16 July 2008 and accepted 20 October 2008, first published online 5 December 2008)

Abstract. We consider an adiabatic dusty plasma containing adiabatic inertialess electrons, adiabatic ions, and adiabatic negatively charged dust. The basic features of the dust–ion-acoustic (DIA) as well as the dust-acoustic (DA) solitary waves (SWs) in such an adiabatic dusty plasma are investigated using the reductive perturbation method, which is valid for small amplitude SWs, and by the pseudo-potential approach which is valid for arbitrary amplitude SWs. The combined effects of the adiabaticity of electrons/ions and negatively charged static/mobile dust on the basic features (polarity, speed, amplitude and width) of small as well as arbitrary amplitude DIA and DA SWs are examined explicitly. It is found that the combined effects of the adiabaticity of electrons/ions and negatively charged static/mobile dust significantly modify the basic features (polarity, speed, amplitude and width) of the DIA and DA SWs. The implications of our results in space and laboratory dusty plasmas are discussed briefly.

1. Introduction

The physics of charged dust particles, which are ubiquitous in space [1–4] and laboratory [4–7] plasmas, has received a great deal of interest in understanding the electrostatic density perturbations and potential structures that are observed in space environments and laboratory devices.

Shukla and Silin [8] have first considered negatively charged static dust, and shown that due to the conservation of equilibrium charge density $n_{e0}e + n_{d0}Z_d e - n_{i0}e = 0$ and the strong inequality $n_{e0} \ll n_{i0}$ (where n_{s0} is the particle number density of the species s with $s = e, i, d$ for electrons, ions, dust, Z_d is the number of electrons residing onto the dust grain surface, and e is the magnitude of the electronic charge) a dusty plasma (with negatively charged static dust grains) supports low-frequency dust–ion-acoustic (DIA) waves with phase speed much smaller (larger) than electron (ion) thermal speed. The dispersion relation (a relation between the wave frequency ω and the wave number k) of the linear DIA waves for the cold ion limit is [8] $\omega^2/k^2 = C_i^2/[(1-\alpha)(1+k^2\lambda_{De}^2)]$, where $C_i = (k_B T_{e0}/m_i)^{1/2}$ is the ion-acoustic speed (with T_{e0} being the electron temperature at equilibrium and m_i being the ion mass, k_B being the Boltzmann constant), $\lambda_{De} = (k_B T_{e0}/4\pi n_{e0} e^2)^{1/2}$ is the electron Debye radius, and $\alpha = Z_d n_{d0}/n_{i0}$. When we consider a long wavelength limit (namely, $k^2\lambda_{De}^2 \ll 1$), the dispersion relation for the DIA waves becomes $\omega/k = C_i/(1-\alpha)^{1/2}$.

This form of spectrum is similar to the usual ion-acoustic wave spectrum for a plasma with $\alpha = 0$ and $T_{i0} \ll T_{e0}$ (where T_{i0} is the ion temperature at equilibrium). However, in dusty plasmas we usually have $\alpha \simeq 1$ and $T_{i0} \simeq T_{e0}$. Therefore, a dusty plasma cannot support the usual ion-acoustic waves, but can support the DIA waves of Shukla and Silin [8]. The DIA waves have been experimentally observed later [9].

On the other hand, it has been shown both theoretically [10] and experimentally [11] that in an unmagnetized dusty plasma the dust charge dynamics introduces a new eigenmode, namely the dust-acoustic (DA) mode [10, 11], whose dispersion relation for a cold dust fluid limit ($T_d = 0$) is given by [10] $\omega^2/k^2 = C_d^2(1-\mu)/(1+\sigma_i\mu + k^2\lambda_{Di}^2)$, where $\lambda_{Di} = (k_B T_{i0}/4\pi n_{i0} e^2)^{1/2}$ is the ion Debye radius, $C_d = (Z_d k_B T_{i0}/m_d)^{1/2}$ is the DA speed, $\mu = n_{e0}/n_{i0}$, and $\sigma_i = T_{i0}/T_{e0}$. Now, if we consider a long wavelength limit (namely $k^2\lambda_{Di}^2 \ll 1$), the dispersion relation for the DA waves becomes $\omega^2/k^2 = C_d^2(1-\mu)/(1+\sigma_i\mu)$. This means that in the DA waves, the dust particle mass provides the inertia and the pressures of inertialess electrons and ions give rise to the restoring force. The linear properties of the DIA and DA waves are now well understood from both theoretical and experimental points of view [3, 4, 8–11].

The nonlinear waves associated with the DIA and DA waves, particularly the DIA and DA SWs, have also received a great deal of interest in understanding the basic properties of localized electrostatic perturbations in space and laboratory dusty plasmas [3, 4, 10, 12–14]. The DIA SWs have been investigated by several authors [12, 15–18]. These works [12, 15–18] are valid only for a cold ions and isothermal (Maxwellian) electrons.

On the other hand, Mamun et al. [19] have investigated the DA SWs [10] in a two-component unmagnetized dusty plasma consisting of a negatively charged cold dust fluid and an inertialess isothermal ion fluid. The work of Mamun et al. [19] is only valid when a complete depletion of electrons onto the dust grain surface is possible. A number of theoretical investigations [20–23] have been made of the DA SWs in order to generalize the work of Mamun et al. [19] by assuming a three-component unmagnetized dusty plasma consisting of a negatively charged cold dust fluid and inertialess isothermal electron and ion fluids. These works are only valid for a cold dust fluid and isothermal electrons and ions. Recently, the effects of the dust fluid temperature on the DA SWs have been investigated by a number of authors [24–27]. Roychoudhury and Mukherjee [24] considered a two-component unmagnetized dusty plasma consisting of a negatively charged adiabatic dust fluid and an inertialess isothermal ion fluid, and investigated the effects of dust fluid temperature on large-amplitude SWs. Mendonza-Briceño et al. [25] assumed a two-component dusty plasma containing the adiabatic dust fluid and non-adiabatic ions following the non-thermal distribution of Cairns et al. [28], and studied the effect of the dust fluid temperature on the DA SWs. Gill et al. [26] assumed a dusty plasma containing the adiabatic dust fluid and non-adiabatic ions following the bi-Maxwellian distribution of Nishihara and Tajiri [29], and studied the effect of the dust fluid temperature on the DA SWs. Sayed and Mamun [27] assumed a dusty plasma containing the adiabatic dust fluid and non-adiabatic (isothermal) inertialess electron and ion fluid, and studied the effect of the dust fluid temperature on the DA SWs. It is obvious that all of these investigations [24–27] are concerned with different dusty plasma models which are not consistent (appropriate) in general. The inconsistency of all of these dusty plasma models arises from the consideration

of one component (dust) being adiabatic, and other components (electrons or ions or both) being non-adiabatic. Therefore, in the present work we consider a consistent dusty plasma model, which assumes a dusty plasma containing non-inertial adiabatic electron fluid, inertial (for DIA waves) and non-inertial (for DA waves) ion fluid and negatively charged inertial adiabatic dust fluid, and perform a proper investigation of the basic properties of the DIA and DA SWs using the reductive perturbation method (RPM), which is valid for small amplitude SWs, and by the pseudo-potential approach (PPA) which is valid for arbitrary amplitude SWs.

The manuscript is organized as follows. The basic equations governing the adiabatic dusty plasma system under consideration are given in Sec. 2. The small as well as arbitrary amplitude DIA SWs are investigated in Sec. 3. The small as well as arbitrary amplitude DA SWs are investigated in Sec. 4. A brief discussion is presented in Sec. 5.

2. Governing equations

We consider the propagation of an electrostatic perturbation mode in an adiabatic dusty plasma containing electrons, ions, and negatively charged dust. The dynamics of a one-dimensional electrostatic perturbation mode in such an adiabatic dusty plasma is governed by

$$\frac{\partial N_s}{\partial T} + \frac{\partial}{\partial X}(N_s U_s) = 0, \tag{1}$$

$$m_s N_s \left(\frac{\partial N_s}{\partial T} + U_s \frac{\partial U_s}{\partial X} \right) = -q_s N_s \frac{\partial \Phi}{\partial X} - \frac{\partial P_s}{\partial X}, \tag{2}$$

$$\frac{\partial P_s}{\partial T} + U_s \frac{\partial P_s}{\partial X} + \gamma_s P_s \frac{\partial U_s}{\partial X} = 0, \tag{3}$$

$$\frac{\partial^2 \Phi}{\partial X^2} = -\sum_s q_s N_s, \tag{4}$$

where N_s is the number density of species s, U_s is the fluid speed, Φ is the wave potential, P_s is the fluid thermal pressure, γ_s is the adiabatic index, m_s is the mass, q_s is the charge, X and T are the space and time variables.

It is important to mention here that for an isothermal process $\gamma_s = 1$ and $P_s = N_s k_B T_s$ with constant T_s (i.e. $T_s = T_{s0}$), and hence (1) and (3) are identical. It is also important to mention that for inertialess isothermal electrons and ions (i.e. for $m_j = 0$, $\gamma_j = 1$, $P_j = N_j k_B T_j$, $T_j = T_{j0}$, where $j = \mathrm{e}$ for the electron fluid and $j = \mathrm{i}$ for the ion fluid), (2) reduces to $N_\mathrm{e} = n_{\mathrm{e}0} \exp(e\Phi/k_B T_\mathrm{e})$ and $N_\mathrm{i} = n_{\mathrm{i}0} \exp(-e\Phi/k_B T_\mathrm{i})$.

3. DIA SWs

We first consider negatively charged static dust ($U_\mathrm{d} = 0$) and non-inertial electrons ($m_\mathrm{e} = 0$), and assume the propagation of the DIA waves [8] whose dynamics is described in terms of the normalized variables as [30]

$$\frac{\partial n_j}{\partial t} + \frac{\partial}{\partial x}(n_j u_j) = 0, \tag{5}$$

$$0 = n_\mathrm{e} \frac{\partial \Psi}{\partial x} - \frac{\partial p_\mathrm{i}}{\partial x}, \tag{6}$$

https://doi.org/10.1017/S0022377808007721 Published online by Cambridge University Press

$$n_{\rm i}\left(\frac{\partial u_{\rm i}}{\partial t}+u_{\rm i}\frac{\partial u_{\rm i}}{\partial x}\right)=-n_{\rm i}\frac{\partial \Psi}{\partial x}-\sigma_{\rm i}\frac{\partial p_{\rm i}}{\partial x}, \tag{7}$$

$$\frac{\partial p_j}{\partial t}+u_j\frac{\partial p_j}{\partial x}+\gamma_j p_j\frac{\partial u_j}{\partial x}=0, \tag{8}$$

$$\frac{\partial^2 \Psi}{\partial x^2}=(1-\alpha)n_{\rm e}-n_{\rm i}+\alpha, \tag{9}$$

where $n_j = N_j/n_{j0}$, $u_j = U_j/C_{\rm i}$, $\Psi = e\Phi/k_{\rm B}T_{\rm e0}$, $p_j = P_j/n_{j0}k_{\rm B}T_{j0}$, $t = T\omega_{\rm pi}$ and $x = X/\lambda_D$ (with $\omega_{\rm pi}^{-1} = (m_{\rm i}/4\pi e^2 n_{\rm i0})^{1/2}$, and $\lambda_{\rm D} = (k_{\rm B}T_{\rm e0}/4\pi e^2 n_{\rm i0})^{1/2}$). We now study small amplitude (SA) DIA SWs by the RPM and arbitrary amplitude (AA) DIA SWs by the PPA.

3.1. SA DIA SWs: RPM

To investigate the basic features of SA DIA SWs by the RPM and the stretched coordinates [33] $\zeta = \epsilon^{1/2}(x - V_{\rm p}t)$ and $\tau = \epsilon^{3/2}t$, where ϵ is a smallness parameter measuring the weakness of the dispersion, and $V_{\rm p}$ is the phase speed (ω/k) of the DIA waves normalized by $C_{\rm i}$, i.e. $V_{\rm p} = \omega/kC_{\rm i}$. We can expand the variables n_j, u_j, p_j and Ψ in power series of ϵ as

$$n_j = 1+\epsilon n_j^{(1)}+\epsilon^2 n_j^{(2)}+\cdots, \tag{10}$$

$$u_j = 0+\epsilon u_j^{(1)}+\epsilon^2 u_j^{(2)}+\cdots, \tag{11}$$

$$p_j = 1+\epsilon p_j^{(1)}+\epsilon^2 p_j^{(2)}+\cdots, \tag{12}$$

$$\Psi = 0+\epsilon \Psi^{(1)}+\epsilon^2 \Psi^{(2)}+\cdots. \tag{13}$$

Now, expressing (5)–(9) in terms of ζ and τ, substituting (10)–(13) into them, one can easily develop different sets of equations in various powers of ϵ. To the lowest order in ϵ one obtains

$$n_{\rm e}^{(1)} = \frac{u_{\rm e}^{(1)}}{V_{\rm p}} = \frac{p_{\rm e}^{(1)}}{\gamma_{\rm e}} = \frac{\Psi^{(1)}}{\gamma_{\rm e}}, \tag{14}$$

$$n_{\rm i}^{(1)} = \frac{u_{\rm i}^{(1)}}{V_{\rm p}} = \frac{p_{\rm i}^{(1)}}{\gamma_{\rm i}} = -\frac{\Psi^{(1)}}{V_{\rm p}^2\left(1-\left(\gamma_{\rm i}\sigma_{\rm i}/V_{\rm p}^2\right)\right)}, \tag{15}$$

$$V_{\rm p}^2 = \frac{\gamma_{\rm e}}{1-\alpha}+\gamma_{\rm i}\sigma_{\rm i}. \tag{16}$$

Equation (16) is the linear dispersion relation for the DIA waves propagating in a dusty plasma under consideration. It is obvious that for isothermal electrons ($\gamma_{\rm e} = 1$) and cold ions ($\sigma_{\rm i} = 0$) the dispersion relation ($\omega/k = C_{\rm i}/\sqrt{1-\alpha}$) is exactly the same as that obtained by Shukla and Silin [8]. We note that $\gamma_{\rm e}$ and $\gamma_{\rm i}$ can vary from one to three, $\sigma_{\rm i}$ can vary from zero to one, and α can vary from zero (dust-free plasma limit) to around one (complete electron depletion). We have numerically shown how the phase speed ($V_{\rm p}$) varies with γ ($=\gamma_{\rm e} = \gamma_{\rm i}$), α and $\sigma_{\rm i}$. The results are displayed in Figs 1 and 2 which indicate that the phase speed $V_{\rm p}$ increases with increasing the values of γ, α and $\sigma_{\rm i}$.

https://doi.org/10.1017/S0022377808007721 Published online by Cambridge University Press

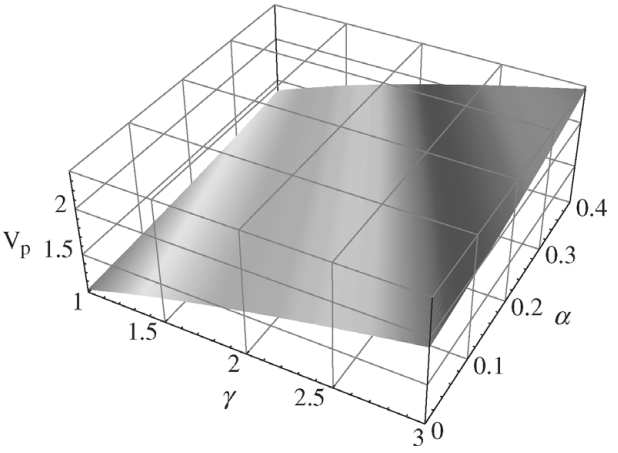

Figure 1. The variation of the phase speed V_p of the DIA waves with γ and α for $\sigma_i = 0.2$.

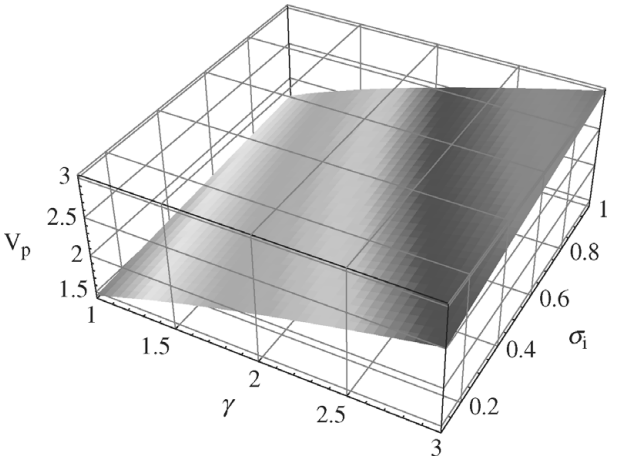

Figure 2. The variation of the phase speed V_p of the DIA waves with γ and σ_i for $\alpha = 0.5$.

Similarly, to the next order in ϵ one obtains another set of equations which, after using (14)–(16), can be reduced to a well-known Korteweg–de Vries (KdV) equation

$$\frac{\partial \Psi^{(1)}}{\partial \tau} + A_i \Psi^{(1)} \frac{\partial \Psi^{(1)}}{\partial \zeta} + B_i \frac{\partial^3 \Psi^{(1)}}{\partial \zeta^3} = 0, \tag{17}$$

where the coefficients A_i and B_i are given by

$$A_i = B_i \left[\frac{1}{V_\sigma^2} \left(3 + \sigma_i \frac{\Gamma_i}{V_\sigma} \right) - \frac{1-\alpha}{\gamma_e^2} \left(3 - \frac{\Gamma_e}{\gamma_e} \right) \right], \tag{18}$$

$$B_i = \frac{V_\sigma^2}{2V_p}, \tag{19}$$

in which $V_\sigma = V_p^2 - \gamma_i \sigma_i$ and $\Gamma_j = \gamma_j(1+\gamma_j)$. Now, transforming the independent variables ζ and τ to $\xi = \zeta - U_0 \tau'$ and $\tau = \tau'$ (where U_0 is a constant velocity normalized by C_i) and imposing the appropriate boundary conditions (namely

https://doi.org/10.1017/S0022377808007721 Published online by Cambridge University Press

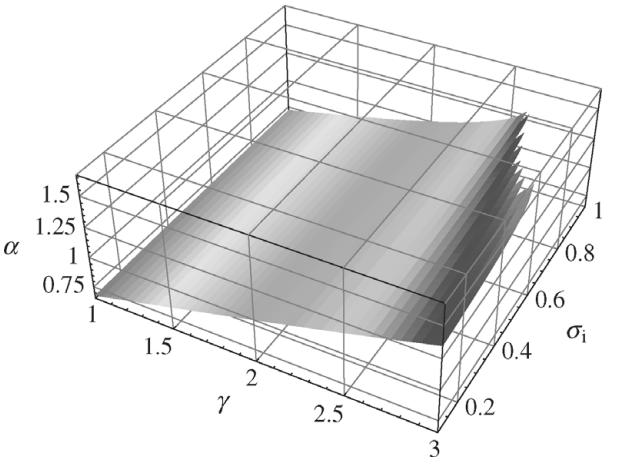

Figure 3. The $A_i = 0$ surface (variation of α with γ and σ_i).

$\Psi^{(1)} \to 0, \partial\Psi^{(1)}/\partial\xi \to 0, \partial^2\Psi^{(1)}/\partial\xi^2 \to 0$ at $\xi \to \pm\infty$), one can express a stationary solitary wave solution of (17) as

$$\Psi^{(1)} = \Psi_m \ \mathrm{sech}^2(\xi/\Delta), \tag{20}$$

where the amplitude Ψ_m (normalized by $k_B T_{e0}/e$) and the width Δ (normalized by λ_D) are given by

$$\Psi_m = \frac{3U_0}{A_i}, \tag{21}$$

$$\Delta = \sqrt{4B_i/U_0}. \tag{22}$$

It is obvious from (20) and (21) that the DIA SWs will be associated with positive (negative) potential when $A_i > 0$ ($A_i < 0$). We, therefore, first analytically analyze the role of the adiabaticity of electrons on changing the polarity of the DIA solitary potential by analyzing A_i for a cold ion limit ($\sigma_i = 0$). This limit allows us to write A_i as $A_i = (1 + \gamma_e - 3\alpha)/2\gamma_e$. This means that the DIA SWs will be associated with positive potential when $\alpha < (1 + \gamma_e)/3$ and with negative potential when $\alpha > (1 + \gamma_e)/3$. This clearly indicates that one cannot have SWs with negative potential for $\gamma_e \geqslant 2$ since α is always less than one. We note that for isothermal electrons ($\gamma_e = 1$) one can have the DIA SWs with positive (negative) potential when $\alpha < 2/3$ ($\alpha > 2/3$). This completely agrees with Bharuthram and Shukla [12] and Mamun and Shukla [15, 16]. To find the parametric regimes for which positive and negative solitary profile exist, we have numerically analyzed A_i and obtain the $A_i = 0$ surface with α, γ and σ_i. The $A_i = 0$ surface is displayed in Fig. 3. We have then graphically shown how the amplitude and the width of the solitary profile vary with different dusty plasma parameters. These are displayed in Figs 4–7. Figure 4 shows that the amplitude of the DIA solitary potential profiles increases with increasing the value of α, but decreases with increasing the value of γ. Figure 5 indicates that the amplitude of the solitary profile decreases with increasing the value of γ and σ_i. It is obvious from Fig. 6 that the width of the solitary potential profiles increases with increasing the values of α and γ. It is found from Fig. 7 that the width decreases with increasing the value of σ_i, but increases with increasing the value of γ.

https://doi.org/10.1017/S0022377808007721 Published online by Cambridge University Press

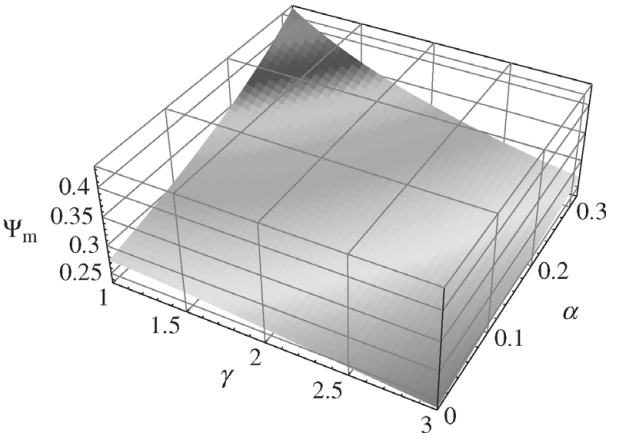

Figure 4. The variation of the amplitude Ψ_m of the DIA solitary wave with γ and α for $\sigma_i = 0.2$ and $U_0 = 0.1$.

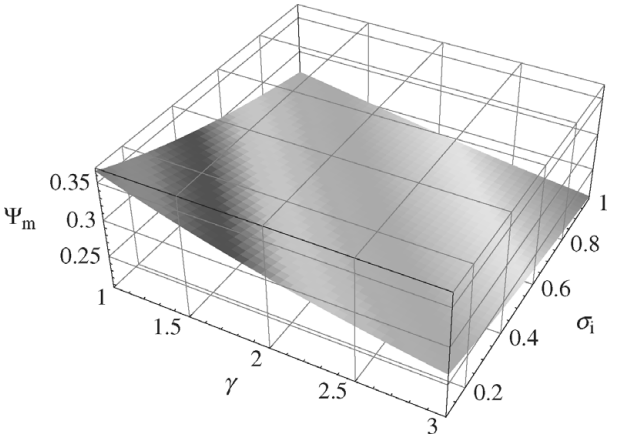

Figure 5. The variation of the amplitude Ψ_m of the DIA solitary wave with γ and σ_i for $\alpha = 0.2$ and $U_0 = 0.1$.

3.2. AA DIA SWs: PPA

To investigate the basic features of the AA DIA SWs by the PPA, we use the transformation $\xi = x - Mt$ (where M is the Mach number, solitary wave speed/C_i), the steady-state condition ($\partial/\partial t = 0$), and the appropriate boundary conditions for localized perturbation (namely $n_j \to 1$, $u_j \to 0$, $p_j \to 1$ and $\Psi \to 0$ at $\xi \to \pm\infty$), which allow us to write (5)–(9) as

$$n_e = \left(1 + \frac{\gamma - 1}{\gamma}\Psi\right)^{1/(\gamma-1)}, \tag{23}$$

$$\gamma_\sigma n_i^{\gamma+1} - (M^2 - 2\Psi + \gamma_\sigma)n_i^2 + M^2 = 0, \tag{24}$$

$$\frac{d^2\Psi}{d\xi^2} = (1-\alpha)n_e - n_i + \alpha, \tag{25}$$

https://doi.org/10.1017/S0022377808007721 Published online by Cambridge University Press

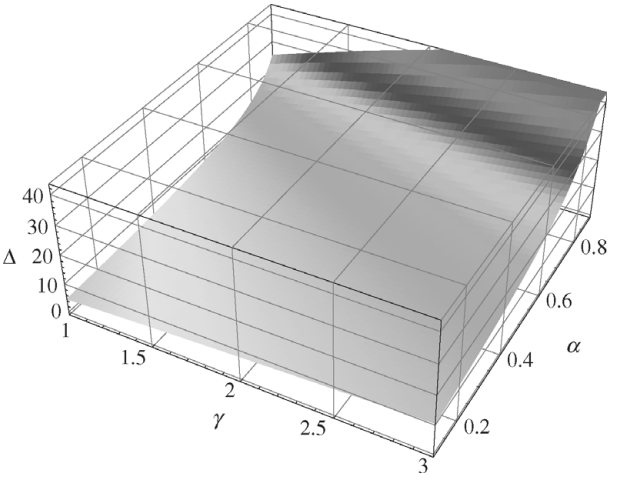

Figure 6. The variation of the width Δ of the DIA solitary wave with γ and α for $\sigma_i = 0.2$ and $U_0 = 0.1$.

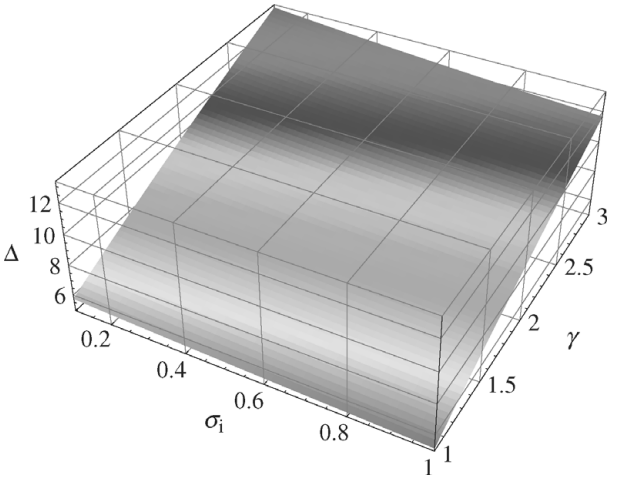

Figure 7. The variation of the width Δ of the DIA solitary wave with γ and σ_i for $\alpha = 0.3$ and $U_0 = 0.1$.

where $\gamma_\sigma = 2\sigma_i\gamma/(\gamma-1)$. It is obvious from (23) and (24) that one cannot substitute $\gamma = 1$ into (23) and (24) directly. Since our present interest is in examining the combined effects of the adiabatic electrons and negatively charged static dust on DIA SWs in an adiabatic dusty plasma, it is sufficient to express (23) and (24) as

$$n_e = \left(1 + \frac{\gamma-1}{\gamma}\Psi\right)^{1/(\gamma-1)}$$

$$\equiv 1 + \left(\frac{1}{\gamma}\right)\Psi + \left(\frac{2-\gamma}{\gamma^2 2!}\right)\Psi^2 + \left[\frac{(3-2\gamma)(2-\gamma)}{\gamma^3 3!}\right]\Psi^3 + \cdots \quad (26)$$

https://doi.org/10.1017/S0022377808007721 Published online by Cambridge University Press

$$n_{\rm i} = \frac{1}{\sqrt{6\sigma_{\rm i}}}\left(\Psi_1 - \sqrt{\Psi_1^2 - 12\sigma_{\rm i}M^2}\right)^{1/2}, \tag{27}$$

where $\Psi_1 = M^2 + 3\sigma_{\rm i} - 2\Psi$. It may be noted here that (26) is valid for both $\gamma = 1$ (which corresponds to $n_{\rm e} = e^{\Phi}$) and $\gamma = 3$ (which corresponds to $n_{\rm e} = (1+2\Phi/3)^{1/2}$). It is obvious from (26) and (27) that one can consider two situations. The first corresponds to $\gamma = 1$ and $\sigma_{\rm i} = 0$ (see [12, 15, 16, 18]) and the other corresponds to $\gamma = 3$ and $\sigma_{\rm i} \neq 0$. The latter is where our present interest lies.

Now, substituting (26) and (27) into (25), multiplying the resulting equation by $d\Psi/d\xi$, and applying the boundary condition, $d\Phi/d\xi \to 0$ at $\xi \to \pm\infty$, one obtains [32]

$$\frac{1}{2}\left(\frac{d\Psi}{d\xi}\right)^2 + V(\Psi) = 0, \tag{28}$$

where $V(\Psi)$ is given by [30]

$$V(\Psi) = C - \alpha\Psi - (1-\alpha)\left(1 + \frac{2}{3}\Psi\right)^{3/2} - \frac{M}{\sqrt{2}}(\Psi_1 + \Psi_2)^{1/2} - 2^{3/2}\sigma_{\rm i}M^3(\Psi_1 + \Psi_2)^{-3/2}, \tag{29}$$

where $C = 1 - \alpha + \sigma_{\rm i} + M^2$ is the integration constant chosen in such a way that $V(\Psi) = 0$ at $\Psi = 0$, and $\Psi_2 = \sqrt{\Psi_1^2 - 12\sigma_{\rm i}M^2}$. Equation (28) can be regarded as an 'energy integral' of an oscillating particle of unit mass, with pseudo-speed $d\Psi/d\xi$, pseudo-position Ψ, pseudo-time ξ and pseudo-potential $V(\Psi)$. This equation is valid for the AA stationary DIA SWs in an adiabatic dusty plasma in the presence of negatively charged static dust. The expansion of $V(\Psi)$ around $\Psi = 0$ is

$$V(\Psi) = -\tfrac{1}{2}C_2\Psi^2 + \tfrac{1}{6}C_3\Psi^3 + \cdots, \tag{30}$$

where

$$C_2 = \frac{1}{3}(1-\alpha) - \frac{1}{M^2 - 3\sigma_{\rm i}}, \tag{31}$$

$$C_3 = -\frac{1}{9}(1-\alpha) + \frac{3(M^2+\sigma_{\rm i})}{(M^2-3\sigma_{\rm i})^3}. \tag{32}$$

It is clear from (30) that $V(\Psi) = dV(\Psi)/d\Psi = 0$ at $\Psi = 0$. Therefore, solitary wave solutions of (28) exist if (i) $(d^2V/d\Psi^2)_{\Psi=0} < 0$, i.e. $C_2 > 0$, so that the fixed point at the origin is unstable, and (ii) $V(\Psi) < 0$ when $0 > |\Psi| > |\Psi_m|$, where $|\Psi_m|$ is a non-zero value of Ψ for which $V(\Psi_m) = 0$, and Ψ_m is the amplitude of the SWs. The condition (i) is satisfied when $M > M_{\rm c}$, where $M_{\rm c} = V_{\rm p}$ and its variation with α and $\sigma_{\rm i}$ is shown in Figs 1 and 2. To examine whether the conditions (i) and (ii) are satisfied simultaneously, $V(\Psi)$ (given in (29)) is numerically analyzed by using typical dusty plasma parameters, namely $\alpha = 0.1$–0.9, $\sigma_{\rm i} = 0.1$–0.9, and $M = M_{\rm c} + 0.1$.

One can easily show by the numerical analysis of $V(\Psi)$ (given in (29)) that the DIA SWs exist only with positive potential ($\Psi > 0$), but not with negative potential ($\Psi < 0$). A part of the numerical analysis, showing the formation of the potential wells in the positive Ψ-axis, i.e. showing the existence of the DIA SWs with $\Psi > 0$, is displayed in Figs 8 and 9.

https://doi.org/10.1017/S0022377808007721 Published online by Cambridge University Press

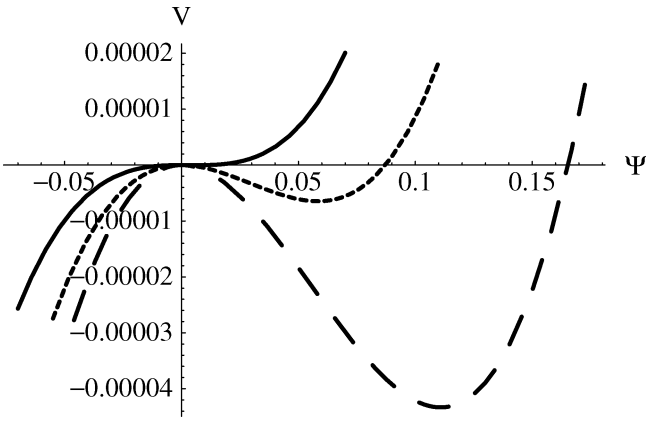

Figure 8. How the potential well starts to form in the positive Ψ-axis when M exceeds $M_c = 1.91$, where $\alpha = 0.1$, $\sigma_i = 0.1$, $M = 1.91$ (solid curve), $M = 1.94$ (dotted curve) and $M = 1.97$ (dashed curve).

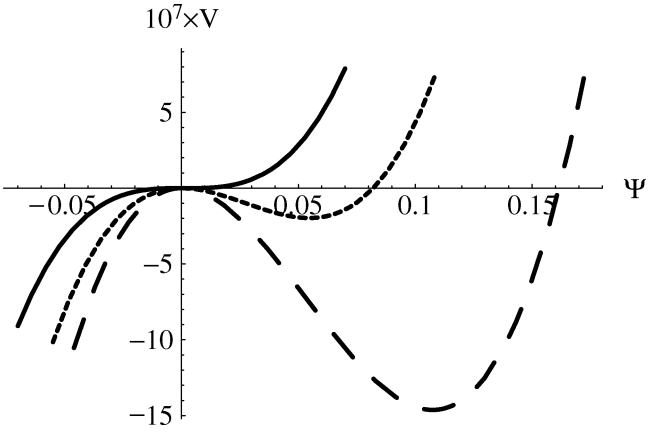

Figure 9. How the potential well starts to form in positive Ψ-axis when M exceeds $M_c = 5.72$, where $\alpha = 0.9$, $\sigma_i = 10^{-3}$, $M = 5.72$ (solid curve), $M = 5.75$ (dotted curve) and $M = 5.78$ (dashed curve).

Figure 8 shows the formation of the potential wells in the positive Ψ-axis, which corresponds to the formation of the DIA SWs with positive potential, for $\alpha = 0.1$, $\sigma_i = 0.1$, $M = 1.91$ (solid curve), $M = 1.94$ (dotted curve) and $M = 1.97$ (dashed curve). Figure 9 shows the formation of the potential wells in the negative Ψ-axis, which corresponds to the formation of SWs with negative potential, for $\alpha = 0.9$, $\sigma_i = 0.9$, $M = 5.72$ (solid curve), $M = 5.75$ (dotted curve) and $M = 5.78$ (dashed curve).

Figures 8 and 9 can also provide a visualization of the amplitude (Ψ_m) and the width ($|\Psi_m|/|V_m|$, where $|V_m|$ is the minimum value of $V(\Psi)$ in the potential wells formed in the positive Ψ-axis). Figures 8 and 9, where the values of M are around its critical value (M_c), indicate the existence of SA DIA SWs. However, in the same way, one can easily show the existence of large-, even extremely large-amplitude DIA SWs just by increasing the value of M. It is found from this visualization

https://doi.org/10.1017/S0022377808007721 Published online by Cambridge University Press

(after a more numerical analysis with different values of α and $\sigma_{\rm i}$, which are not shown) that the variation of the amplitude and the width with α and $\sigma_{\rm i}$ in the case of AA DIA SWs are exactly the same as that in the case of SA DIA SWs.

4. DA SWs

We next consider the negatively charged mobile dust (i.e. $U_{\rm d} \neq 0$) and non-inertial electrons and ions ($m_{\rm e} = 0$ and $m_{\rm i} = 0$), and assume the propagation of the DA waves [10] whose dynamics is described in terms of normalized variables as [31]

$$\frac{\partial n_s}{\partial t} + \frac{\partial}{\partial x}(n_s u_s) = 0, \tag{33}$$

$$\frac{\partial p_s}{\partial t} + u_s \frac{\partial p_s}{\partial x} + \gamma p_s \frac{\partial u_s}{\partial x} = 0, \tag{34}$$

$$\frac{\partial p_{\rm e}}{\partial x} = n_{\rm e}\sigma_{\rm i}\frac{\partial \Psi}{\partial x}, \tag{35}$$

$$\frac{\partial p_{\rm i}}{\partial x} = -n_{\rm i}\frac{\partial \Psi}{\partial x}, \tag{36}$$

$$\frac{\partial u_{\rm d}}{\partial t} + u_{\rm d}\frac{\partial u_{\rm d}}{\partial x} = \frac{\partial \Psi}{\partial x} - \frac{\sigma_{\rm d}}{n_{\rm d}}\frac{\partial p_{\rm d}}{\partial x}, \tag{37}$$

$$\frac{\partial^2 \Psi}{\partial x^2} = \mu_{\rm e} n_{\rm e} - \mu_{\rm i} n_{\rm i} + n_{\rm d}, \tag{38}$$

where $n_s = N_s/n_{s0}$, $u_s = U_s/C_{\rm d}$, $\Psi = e\Phi/k_{\rm B}T_{\rm i0}$, $p_s = P_s/n_{s0}k_{\rm B}T_{s0}$, $t = T\omega_{\rm pd}$, $x = X/\lambda_{\rm Dm}$ (with $\omega_{\rm pd}^{-1} = (m_{\rm d}/4\pi Z_{\rm d}^2 e^2 n_{\rm d0})^{1/2}$ and $\lambda_{\rm Dm} = (k_{\rm B}T_{\rm i0}/4\pi Z_{\rm d} n_{\rm d0} e^2)^{1/2}$), $\sigma_{\rm d} = T_{\rm d0}/Z_{\rm d}T_{\rm i0}$, $\mu = n_{\rm e0}/n_{\rm i0}$, $\mu_{\rm e} = \mu/(1-\mu)$, and $\mu_{\rm i} = 1/(1-\mu)$.

It is important to note that for isothermal processes, (35) and (36) reduce to $n_{\rm e} = \exp(\Psi/\sigma_{\rm i})$ and $n_{\rm i} = \exp(-\Psi)$ which are used by Mendonza-Briceño et al. [25], Gill et al. [26] and Sayed and Mamun [27]. To consider an adiabatic dusty plasma, one cannot use $\gamma = 1$ and $p_s = n_s$ with constant T_s. We now study SA DA SWs by the RPM and AA DA SWs by the PPA.

4.1. SA DA SWs: RPM

To investigate the basic features of SA DA SWs by the reductive perturbation technique and the stretched coordinates [33] $\zeta = \epsilon^{1/2}(x - V_0 t)$ and $\tau = \epsilon^{3/2}t$, where ϵ is a smallness parameter measuring the weakness of the dispersion, and V_0 is the phase speed (ω/k) of the DA waves normalized by $C_{\rm d}$, i.e. $V_0 = \omega/kC_{\rm d}$. We can expand the variables n_s, u_s, p_s, and Ψ in power series of ϵ as

$$n_s = 1 + \epsilon n_s^{(1)} + \epsilon^2 n_s^{(2)} + \cdots, \tag{39}$$

$$u_s = 0 + \epsilon u_s^{(1)} + \epsilon^2 u_s^{(2)} + \cdots, \tag{40}$$

$$p_s = 1 + \epsilon p_s^{(1)} + \epsilon^2 p_s^{(2)} + \cdots, \tag{41}$$

$$\Psi = 0 + \epsilon \Psi^{(1)} + \epsilon^2 \Psi^{(2)} + \cdots. \tag{42}$$

Now, expressing (33)–(38) in terms of ζ and τ, substituting (39)–(42) into (33)–(38), one can easily develop different sets of equations in various powers of ϵ. To the

https://doi.org/10.1017/S0022377808007721 Published online by Cambridge University Press

lowest order in ϵ one obtains

$$n_{\rm e}^{(1)} = \frac{u_{\rm e}^{(1)}}{V_0} = \frac{p_{\rm e}^{(1)}}{\gamma} = \sigma_{\rm i}\frac{\Psi^{(1)}}{\gamma}, \tag{43}$$

$$n_{\rm i}^{(1)} = \frac{u_{\rm i}^{(1)}}{V_0} = \frac{p_{\rm i}^{(1)}}{\gamma} = -\frac{\Psi^{(1)}}{\gamma}, \tag{44}$$

$$n_{\rm d}^{(1)} = \frac{u_{\rm d}^{(1)}}{V_0} = \frac{p_{\rm d}^{(1)}}{\gamma} = \frac{\Psi^{(1)}}{\sigma_{\rm d}\gamma - {V_0}^2}, \tag{45}$$

$$V_0^2 = \gamma\left(\sigma_{\rm d} + \frac{1-\mu}{\sigma_{\rm i}\mu + 1}\right). \tag{46}$$

Equation (46) is the linear dispersion relation for the DA waves propagating in a dusty plasma under consideration. It implies that for inertialess isothermal electrons and ions ($\gamma = 1$) and cold dust fluid ($\sigma_{\rm d} = 0$), the phase speed ($\omega/k = C_{\rm d}\sqrt{(1-\mu)/(1+\sigma_{\rm i}\mu)}$) is exactly the same as obtained by Rao [10] and Mamun [21]. We note that $1 \leqslant \gamma \leqslant 3$, $0 < \sigma_{\rm i} \leqslant 1$ and $0 \leqslant \mu < 1$. Therefore, owing to the adiabaticity of electrons and ions, the phase speed of the DA waves can be increased significantly.

Similarly, to the next order in ϵ one obtains another set of equations which, after using (43)–(46), can be reduced to a well-known KdV equation

$$\frac{\partial\Psi^{(1)}}{\partial\tau} + A_{\rm d}\Psi^{(1)}\frac{\partial\Psi^{(1)}}{\partial\zeta} + B_{\rm d}\frac{\partial^3\Psi^{(1)}}{\partial\zeta^3} = 0, \tag{47}$$

where the coefficients $A_{\rm d}$ and $B_{\rm d}$ are given by

$$A_{\rm d} = -B_{\rm d}\left[\Gamma\left(\mu_{\rm e}\sigma_{\rm i}^2 - \mu_{\rm i}\right) + \frac{1}{V_\mu^6}\left(3V_\mu^2 + \Gamma_\sigma\right)\right], \tag{48}$$

$$B_{\rm d} = \frac{V_\mu^4}{2V_0}, \tag{49}$$

in which $V_\mu^2 = \gamma(1-\mu)/(1+\sigma_{\rm i}\mu)$, $\Gamma = (2-\gamma)/\gamma^2$, and $\Gamma_\sigma = \sigma_{\rm d}\gamma(1+\gamma)$.

Now, transforming the independent variables ζ and τ to $\xi = \zeta - U_0\tau'$ and $\tau = \tau'$ (where U_0 is a constant velocity normalized by $C_{\rm d}$) and imposing the appropriate boundary conditions (namely $\Psi^{(1)} \to 0$, $\partial\Psi^{(1)}/\partial\xi \to 0$, $\partial^2\Psi^{(1)}/\partial\xi^2 \to 0$ at $\xi \to \pm\infty$), one can express the stationary solution of the KdV equation (47) as

$$\Psi^{(1)} = \Psi_0\ {\rm sech}^2(\xi/\delta), \tag{50}$$

where the amplitude Ψ_m (normalized by $k_{\rm B}T_{\rm i0}/e$) and the width δ (normalized by $\lambda_{\rm Dm}$) are given by

$$\Psi_0 = \frac{3U_0}{A_{\rm d}}, \tag{51}$$

$$\delta = \sqrt{4B_{\rm d}/U_0}. \tag{52}$$

It is obvious from (50) and (51) that the DA SWs will be associated with positive (negative) potential when $A_{\rm d} > 0$ ($A_{\rm d} < 0$). We note that for isothermal electrons and ions ($\gamma = 1$) and cold dust fluid ($\sigma_{\rm d} = 0$), we can express $A_{\rm d}$ as $A_{\rm d} = -[V_0/$

https://doi.org/10.1017/S0022377808007721 Published online by Cambridge University Press

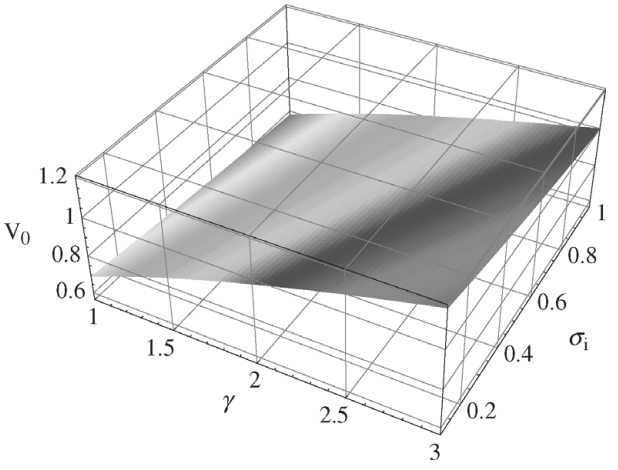

Figure 10. The variation of the phase speed V_0 of the DA waves with γ and σ_i for $\sigma_d = 0.0001$ and $\mu = 0.5$.

$(1-\mu)^2][1+(3+\sigma_i\mu)\sigma_i\mu+\mu(1+\sigma_i^2)/2]$ which is always negative. This means that for isothermal electrons and ions ($\gamma = 1$) and cold dust fluid ($\sigma_d = 0$) DA SWs exist only with negative potential. This agrees completely with Mamun [21]. To include the effects of the adiabaticity of electrons and ions on the polarity of the DA solitary wave potential, we numerically analyze A_d, and find that A_d is always negative. This means that the DA SWs are associated only with the negative potential, and that the effects of the adiabaticity of electrons and ions do not have any role in changing the polarity of the solitary potential. However, these can have a significant role in modifying the other basic properties (namely speed, amplitude and width) of the DA SWs. These are displayed in Figs 10–15. Figures 10 and 11 show that the DW SW speed (V_0) increases with γ, but decreases with μ and σ_i. Figures 12 and 13 indicate that the magnitude of the DW SW amplitude ($|\Psi_m|$) increases with γ, but decreases with μ and σ_i. It is obvious from Figs 14 and 15 that the DW SW width (δ) increases with γ, but decreases with μ and σ_i. It is clear from Figs 11, 13 and 15 that the dust fluid temperature does not have any significant role in modifying the basic features of the DA SWs.

4.2. AA DA SWs: PPA

To study the AA DA SWs for $\gamma = 3$ and $\sigma_d \neq 0$, we use transformation $\xi = x - Mt$ (where M is the Mach number, solitary wave speed/C_d), the steady-state condition ($\partial/\partial t = 0$) and the appropriate boundary conditions for localized perturbations (namely $n_s \to 1$, $u_s \to 0$, $p_s \to 1$ and $\Psi \to 0$ at $\xi \to \pm\infty$) in (33)–(37). These allow us to express n_e, n_i and n_d as

$$n_e = \left(1 + \frac{2}{3}\sigma_i\Psi\right)^{1/2}, \tag{53}$$

$$n_i = \left(1 - \frac{2}{3}\Psi\right)^{1/2}, \tag{54}$$

$$n_d = \frac{M_\sigma}{\sqrt{6\sigma_d}}(\Psi_1 - \Psi_2)^{1/2}, \tag{55}$$

https://doi.org/10.1017/S0022377808007721 Published online by Cambridge University Press

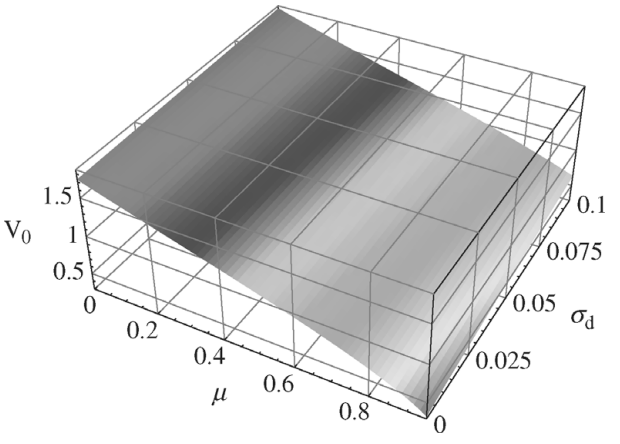

Figure 11. The variation of the phase speed V_0 of the DA waves with μ and σ_d for $\sigma_i = 0.5$ and $\gamma = 3$.

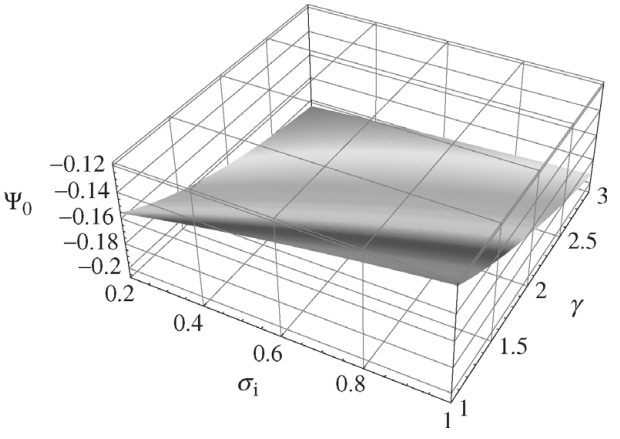

Figure 12. The variation of the amplitude Ψ_0 of the DA SWs with σ_i and γ for $\sigma_d = 0.0001$ and $\mu = 0.5$.

where $\Psi_1 = 1 + 2\Psi/M_\sigma^2$, $\Psi_2 = \sqrt{\Psi_1^2 - 12\sigma_d M^2/M_\sigma^4}$, and $M_\sigma = (M^2 + 3\sigma_d)^{1/2}$. Again, using the transformation $\xi = x - Mt$, substituting (53)–(55) into (38), multiplying the resulting equation by $d\Psi/d\xi$, and applying the boundary condition, $d\Phi/d\xi \to 0$ at $\xi \to \pm\infty$, one obtains [32]

$$\frac{1}{2}\left(\frac{d\Psi}{d\xi}\right)^2 + V(\Psi) = 0, \tag{56}$$

where $V(\Psi)$ is given by [31]

$$V(\Psi) = C - \frac{\mu_e}{\sigma_i}\left(1 + \frac{2}{3}\sigma_i\Psi\right)^{3/2} - \mu_i\left(1 - \frac{2}{3}\Psi\right)^{3/2} - \frac{M}{\sqrt{2}}M_\sigma(\Psi_1 + \Psi_2)^{1/2} - 2^{3/2}\sigma_d\frac{M^3}{M_\sigma^3}(\Psi_1 + \Psi_2)^{-3/2}, \tag{57}$$

https://doi.org/10.1017/S0022377808007721 Published online by Cambridge University Press

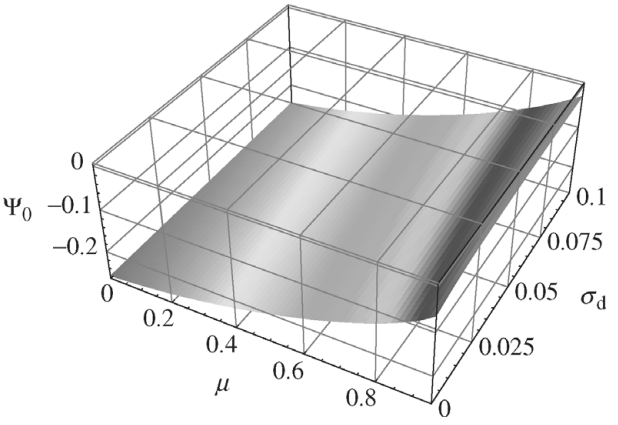

Figure 13. The variation of the amplitude Ψ_0 of the DA SWs with μ and σ_d for $\sigma_i = 0.5$ and $\gamma = 3$.

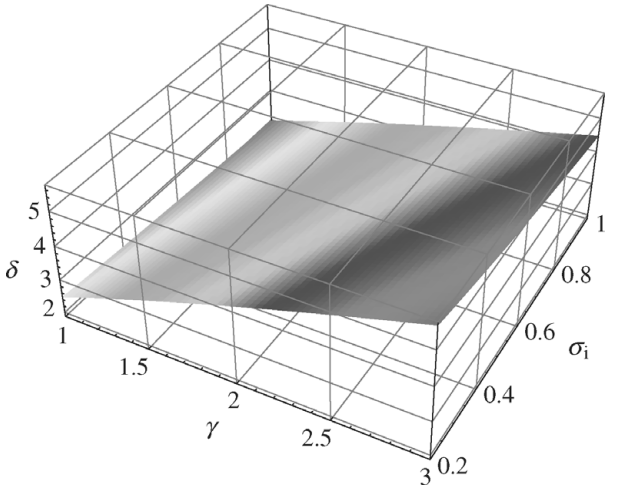

Figure 14. The variation of the width δ of the DA SWs with γ and σ_i for $\sigma_d = 0.0001$ and $\mu = 0.5$.

where the integration constant $C = \mu_e/\sigma_i + \mu_i + \sigma_d + M^2$ is chosen in such a way that $V(\Psi) = 0$ at $\Psi = 0$. Equation (56) can be regarded as an 'energy integral' of an oscillating particle of unit mass, with pseudo-speed $d\Psi/d\xi$, pseudo-position Ψ, pseudo-time ξ and pseudo-potential $V(\Psi)$. This equation is valid for AA stationary DA SWs in an adiabatic hot dusty plasma. The expansion of $V(\Psi)$ around $\Psi = 0$ is

$$V(\Psi) = C_2\Psi^2 + C_3\Psi^3 + \cdots, \tag{58}$$

where

$$C_2 = \frac{1}{2}\left[\frac{1}{M^2 - 3\sigma_d} - \frac{1 + \sigma_i\mu}{3(1-\mu)}\right], \tag{59}$$

$$C_3 = -\frac{1}{6}\left[\frac{3(M^2 + \sigma_d)}{(M^2 - 3\sigma_d)^3} + \frac{1 - \sigma_i^2\mu}{9(1-\mu)}\right]. \tag{60}$$

https://doi.org/10.1017/S0022377808007721 Published online by Cambridge University Press

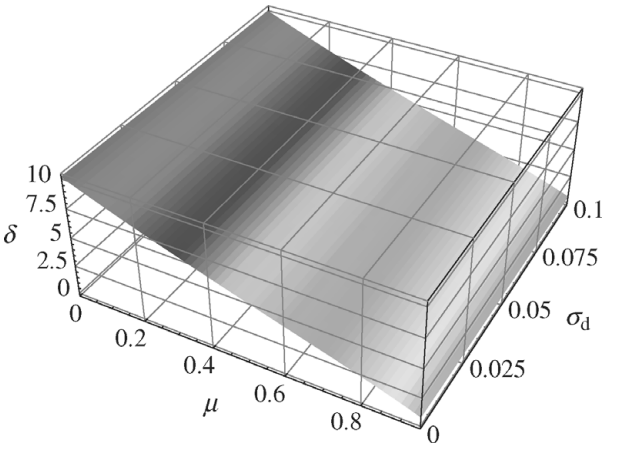

Figure 15. The variation of the width δ of the DA SWs with μ and $\sigma_{\rm d}$ for $\sigma_{\rm i} = 0.5$ and $\gamma = 3$.

It is clear from (58) that $V(\Psi) = dV(\Psi)/d\Psi = 0$ at $\Psi = 0$. Therefore, solitary wave solutions of (56) exist if (i) $(d^2V/d\Psi^2)_{\Psi=0} < 0$, i.e. $C_2 < 0$, so that the fixed point at the origin is unstable, and (ii) $V(\Psi) < 0$ when $0 > |\Psi| > |\Psi_m|$, where $|\Psi_m|$ is a non-zero value of Ψ for which $V(\Psi_m) = 0$, and Ψ_m is the amplitude of the SWs. The condition (i) is satisfied when $M > M_{\rm c}$, where $M_{\rm c} = V_0$ is defined by (46) and its variation with μ, $\sigma_{\rm i}$ and $\sigma_{\rm d}$ are shown in Figs 10 and 11. To examine whether the conditions (i) and (ii) are satisfied simultaneously, $V(\Psi)$ (given in (57)) is numerically analyzed by using typical plasma parameters, namely $\mu = 0.1 - 0.9$, $\sigma_{\rm i} = 0.1 - 0.9$, $\sigma_{\rm d} = 10^{-5} - 10^{-3}$, and $M > M_{\rm c}$.

One can easily show by the numerical analysis of $V(\Psi)$ (given in (57)) that the DA SWs exist only with negative potential ($\Psi < 0$), but not with positive potential ($\Psi > 0$). A part of the numerical analysis, showing the formation of the potential wells in the negative Ψ-axis, i.e. showing the existence of the DA SWs with negative potential, is displayed in Figs 16 and 17. Figure 16 shows the formation of the potential wells in the negative Ψ-axis, which corresponds to the formation of the DA SWs with negative potential, for $\mu = 0.1$, $\sigma_{\rm i} = 0.1$, $\sigma_{\rm d} = 10^{-5}$, $M = 1.64$ (solid curve), $M = 1.67$ (dotted curve) and $M = 1.70$ (dashed curve). Figure 17 shows the formation of the potential wells in the negative Ψ-axis, which corresponds to the formation of SWs with negative potential, for $\mu = 0.9$, $\sigma_{\rm i} = 0.9$, $\sigma_{\rm d} = 10^{-3}$, $M = 0.42$ (solid curve), $M = 0.44$ (dotted curve) and $M = 0.46$ (dashed curve). Figures 16 and 17 can also provide a visualization of the amplitude (Ψ_m) and the width ($|\Psi_m|/|V_m|$, where $|V_m|$ is the minimum value of $V(\Psi)$ in the potential wells formed in the negative Ψ-axis). Figures 16 and 17, where the values of M are around its critical value ($M_{\rm c}$), indicate the existence of SA DA SWs. However, in the same way, one can easily show the existence of large-, even extremely large-amplitude DA SWs just by increasing the value of M. It is found from this visualization (after a more numerical analysis with different values of μ and $\sigma_{\rm i}$, which are not shown) that the variation of the amplitude and the width with μ and $\sigma_{\rm i}$ in the case of AA DA SWs are exactly the same as that in the case of SA DA SWs.

https://doi.org/10.1017/S0022377808007721 Published online by Cambridge University Press

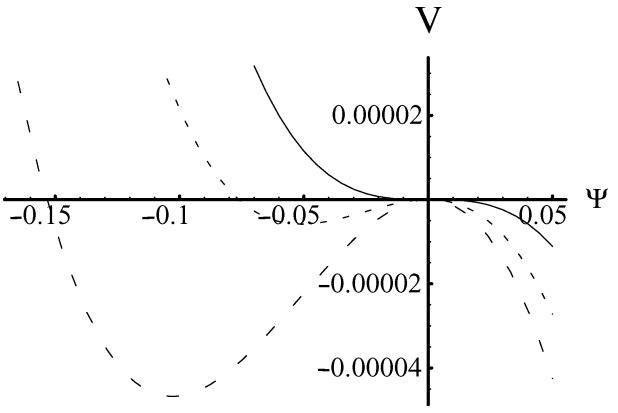

Figure 16. How the potential well starts to form in the negative Ψ-axis when M exceeds $M_c = 1.635$, where $\mu = 0.1$, $\sigma_i = 0.1$, $\sigma_d = 10^{-5}$, $M = 1.64$ (solid curve), $M = 1.67$ (dotted curve) and $M = 1.70$ (dashed curve).

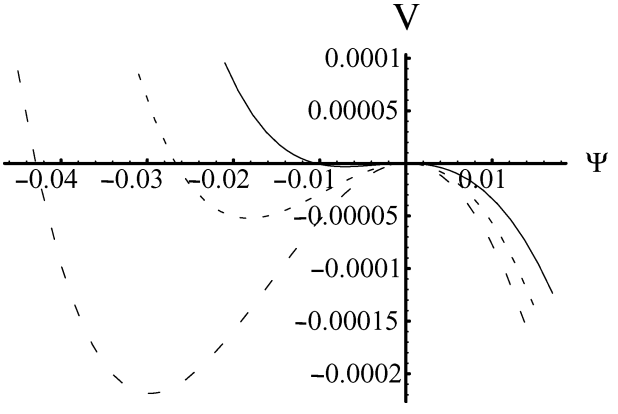

Figure 17. How the potential well starts to form in the negative Ψ-axis when M exceeds $M_c = 0.411$, where $\mu = 0.9$, $\sigma_i = 0.9$, $\sigma_d = 10^{-3}$, $M = 0.42$ (solid curve), $M = 0.44$ (dotted curve) and $M = 0.46$ (dashed curve).

5. Discussion

We have considered a consistent and realistic dusty plasma system containing non-inertial adiabatic electrons and inertial (in the case of DIA SWs) or non-inertial (in the case of DA SWs) ions, and negatively charged static (in the case of DIA SWs) or mobile (in the case of DA SWs) dust, and performed a proper investigation of the basic properties of DIA and DA SWs by the RPM [33] and PPA [32]. The results that we have found in this investigation can be summarized as follows.

1. The effects of adiabatic electrons, negatively charged static dust and adiabatic ion-temperature significantly modify the basic properties (speed, amplitude and width) of the DIA KdV solitons.

2. The effect of the adiabatic electrons kills the possibility of the formation of the negative DIA SWs for any possible set of plasma parameters ($0 \leqslant \sigma_i < 1$ and $0 \leqslant \sigma_i \leqslant 1$).

https://doi.org/10.1017/S0022377808007721 Published online by Cambridge University Press

3. It is obvious that for $\gamma_e = 1$ and $\sigma_i = 0$ the DIA SWs obtained in this investigation agree completely with Bharuthram and Shukla [12] and Mamun and Shukla [15, 16].

4. The effects of adiabaticity of electrons and ions significantly modify the basic properties (speed, amplitude and width) of the DA KdV solitons.

5. It is found that the effects of the adiabatic electrons and ions do not have any role in changing the polarity of the DA SWs for any possible set of plasma parameters ($1 \leqslant \gamma \leqslant 3$, $0 < \sigma_i \leqslant 1$ and $0 \leqslant \mu < 1$).

6. It may be noted that for $\gamma = 1$ and $\sigma_d = 0$ the basic features of the DA SWs found in the present investigation agree completely with Rao [10] and Mamun [21].

The ranges of different plasma parameters used in this investigation are very wide ($\sigma_i = 0.1$–0.9 and $\sigma_i = 0.1$–0.9), and are relevant to both space [1–4] and laboratory [4, 6, 7] plasmas. Thus, the results of the present investigation should help us to explain the basic features of the localized electro-acoustic perturbations propagating in space [1–4] and laboratory [4, 6, 7] dusty plasmas.

References

[1] Goertz, C. K. 1989 *Rev. Geophys.* **27**, 271.
[2] Mendis, D. A. and Rosenberg, M. 1994 *Annu. Rev. Astron. Astrophys.* **32**, 419.
[3] Verheest, F. 2000 *Waves in Dusty Plasmas*. Dordrecht: Kluwer.
[4] Shukla, P. K. and Mamun, A. A. 2002 *Introduction to Dusty Plasma Physics*. Bristol: Institute of Physics.
[5] Ishihara, O. 2007 *J. Phys.* D **40**, R121.
[6] Selwyn, G. S. 1993 *Jpn. J. Appl. Phys.* **32**, 3068.
[7] Winter, J. 1998 *Plasma Phys. Control. Fusion* **340**, 1201.
[8] Shukla, P. K. and Silin, V. P. 1992 *Phys. Scripta* **45**, 508.
[9] Barkan, A., D'Angelo, N. and Merlino, R. L. 1996 *Planet. Space Sci.* **44**, 239.
[10] Rao, N. N., Shukla, P. K. and Yu, M. Y. 1990 *Planet. Space Sci.* **38**, 543.
[11] Barkan, A., Merlino, R. L. and D'Angelo, N. 1995 *Phys. Plasmas* **2**, 3563.
[12] Bharuthram, R. and Shukla, P. K. 1992 *Planet. Space Sci.* **40**, 973.
[13] Nakamura, Y., Bailung, H. and Shukla, P. K. 1999 *Phys. Rev. Lett.* **83**, 1602.
[14] Nakamura, Y. and Sharma, A. 2001 *Phys. Plasmas* **8**, 3921.
[15] Mamun, A. A. and Shukla, P. K. 2002 *Phys. Plasmas* **9**, 1470.
[16] Mamun, A. A. and Shukla, P. K. 2002 *IEEE Trans. Plasma Sci.* **30**, 720.
[17] Shukla, P. K. and Mamun, A. A. 2003 *New J. Phys.* **5**, 17.1.
[18] Mamun, A. A. and Shukla, P. K. 2005 *Plasma Phys. Contr. Fusion* **47**, A1–49.
[19] Mamun, A. A., Shukla, P. K. and Cairns, R. A. 1996 *Phys. Plasmas* **3**, 702.
[20] Ma, J. X. and Liu, J. 1997 *Phys. Plasmas* **4**, 253.
[21] Mamun, A. A. 1999 *Astrophys. Space Sci.* **268**, 443.
[22] Mamun, A. A. and Shukla, P. K. 2001 *Phys. Lett.* A **290**, 173.
[23] Mamun, A. A. and Shukla, P. K. 2002 *Phys. Scripta* **T98**, 107.
[24] Roychoudhury, R. and Mukkerjee, S. 1997 *Phys. Plasmas* **4**, 2305.
[25] Mendoza-Briceño, C. A. et al. 2000 *Planet. Space Sci.* **48**, 599.
[26] Gill, T. S., Kaur, H. and Saini, N. S. 2004 *J. Plasma Phys.* **70**, 481.

[27] Sayed, F. and Mamun, A. A. 2007 *Phys. Plasmas* **14**, 014502.
[28] Cairns, R. A. et al. 1995 *Geophys. Res. Lett.* **22**, 2709.
[29] Nishihara, K. and Tajiri, M. 1981 *J. Phys. Soc. Japan* **50**, 4047.
[30] Mamun, A. A. 2008 *Phys. Lett.* A **372**, 1490.
[31] Mamun, A. A. 2008 *Phys. Lett.* A **372**, 884.
[32] Bernstein, I. B., Greene, J. M. and Kruskal, M. D. 1957 *Phys. Rev.* **108**, 546.
[33] Washimi, H. and Taniuti, T. 1966 *Phys. Rev. Lett.* **17**, 996.